NJC

PAPER

View Article Online
View Journal | View Issue

Cite this: *New J. Chem.*, 2015, 39, 5395

Grain size effect on magnetic and phase transition features in one-dimensional S = 1/2 Heisenberg spin chain molecular crystals†

Guo-Jun Yuan,[ab] Yun-Xia Sui,*[c] Jian-Lan Liu[ab] and Xiao-Ming Ren*[abd]

Received (in NJQUE)
21st March 2015,
Accepted 20th April 2015

DOI: 10.1039/c5nj00709g

www.rsc.org/njc

In this study, we prepared sub-micron crystals of one-dimensional (1D) spin-Peierls-type compounds, 1-(4′-R-benzyl)pyridinium-d_5 bis(maleonitriledithiolato)nickelate (R = Br or Cl), using a facile method, namely, an acetonitrile solution of each compound was quickly mixed with excess water (an insoluble solvent). This facile method of preparation gave a uniform dispersion of sub-micron crystals with a typical dimension of <1.0 μm. We observed that the reduction in grain size affected the magnetic and phase transition features. With respect to the bulk crystal samples, the powder X-ray diffraction peaks are broadened, the transition temperature (T_C) is up-shifted with $\Delta T_C \approx 1.2$ K for R = Br *vs.* 1.0 K for R = Cl, and the changes of enthalpy and entropy of the phase transition are significantly decreased for the sub-micron crystal samples; in addition, reducing the crystal grain size leads to the onset of a strongly Curie–Weiss-type paramagnetic background and significant temperature-independent paramagnetism.

Introduction

Inorganic crystals, which consist of a network of ordered atoms or ions without a discernible molecular unit, generally show size-dependent electronic properties,[1–3] thought to originate from phonon confinement, additional surface phonons or tensile surface stresses.[4] However, molecular crystals usually exhibit size-independent electronic properties because molecules are localized entities; the weak intermolecular interactions rarely extend beyond the nearest neighbors in a typical molecular crystal and enable the bulk properties of a molecular crystal to regularly be analyzed as the sum of individual molecular contributions, with small perturbations from the intermolecular forces.[5] This is one of the main reasons, in the context of molecular crystals, that the study of size-dependent electronic properties has received relatively little attention so far. It is possible that molecular crystals display size-dependent electronic or magnetic behavior if there are non-ignorable electron–phonon/spin–phonon interactions.

In previous studies, we designed and achieved a series of 1D $[Ni(mnt)_2]^-$-based spin-Peierls-type molecular crystals (mnt^{2-} = maleonitriledithiolate),[6] and observed local structural fluctuation in these magnetic chain systems, which is a typical phenomenon originating from electron–phonon or magnetoelastic coupling interactions.[7] This has motivated us to further investigate the magnetic and phase transition natures of such spin-Peierls-type molecular crystals at the nano-scale/sub-micron scale, to gain new evidence of magnetoelastic interactions.

In this paper, sub-micron crystals of two 1D $[Ni(mnt)_2]^-$-based spin-Peierls-type compounds, the molecular structure of which is illustrated in Scheme 1, were prepared using a facile method. The sub-micron crystals of these 1D spin-Peierls-type

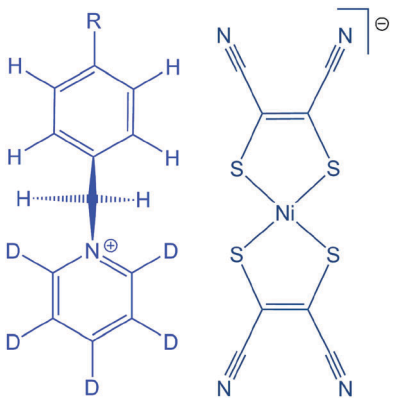

Scheme 1 Molecular structure of 1-(4′-R-benzyl)pyridinium-d_5 bis(maleonitriledithiolato)nickelate (R = Br or Cl).

[a] State Key Laboratory of Materials-Oriented Chemical Engineering and College of Science, Nanjing Tech University, Nanjing 210009, P. R. China. E-mail: xmren@njtech.edu.cn; Fax: +86 25 58130481; Tel: +86 25 58130476
[b] College of Materials Science & Engineering, Nanjing Tech University, Nanjing 210009, P. R. China
[c] Centre of Modern Analysis, Nanjing University, Nanjing 210093, P. R. China. E-mail: suiyx@163.com
[d] State Key Laboratory of Coordination Chemistry, Nanjing University, Nanjing 210093, P. R. China

† Electronic supplementary information (ESI) available: The theoretical and experimental χ_m–T plots and the SEM images of Br-2 and Cl-2 prepared in different batches are included. See DOI: 10.1039/c5nj00709g

transition compounds display that the spin-Peierls-type transition, T_C, up shifts and the magnetic susceptibility shows more gradual change around T_C with respect to the bulk crystals.

Experimental section

Chemicals and materials

All reagents and chemicals were purchased from commercial sources and used without further purification. The compounds 1-(4′-R-benzyl)pyridinium-d_5 bis(maleonitriledithiolato)nickelate (R = bromo and chloro; abbreviated as Br-1 and Cl-1, respectively) and their bulk crystals were obtained by means of a previously reported approach.[8]

Preparation of sub-micron crystals

400 mL of water, an insoluble solvent, was quickly added to 10 mL of an acetonitrile solution with 595 mg (1.0 mmol) of 1-(4′-bromobenzyl)pyridinium-d_5 bis(maleonitriledithiolato)-nickelate. The mixture was vigorously stirred at ambient temperature for 20 min, followed by standing for 10 hours; the precipitate was filtered off using a superfine fiber filter membrane and dried under vacuum. The sub-micron crystals were labeled as Br-2.

A similar procedure was utilized for the preparation of sub-micron crystals of 1-(4′-chlorobenzyl)pyridinium-d_5 bis(maleonitrile-dithiolato)nickelate, and the corresponding sample was labeled as Cl-2.

Physical measurements

Powder X-ray diffraction (PXRD) data were collected using a Bruker D8 Advance powder diffractometer operating at 40 kV and 40 mA, using Cu Kα radiation with λ = 1.5418 Å. Samples were scanned in the range of 2θ = 5–50° with 0.02° per step and 1.2 s per step. The morphology and crystal grain sizes of the samples were observed using a Hitachi S-3400N-II scanning electron microscope at an operating voltage of 15 kV. Magnetic susceptibility data were measured over the temperature range of 2–300 K using a Quantum Design MPMS-5S superconducting quantum interference device (SQUID) magnetometer. Differential scanning calorimetry (DSC) was carried out using a Q2000 V24.9 Build 121 instrument in the temperature range of 93–293 K (from −180 to 20 °C) with a rate of 20 K min^{-1}.

Results and discussion

SEM images and PXRD patterns

Fig. 1 shows the scanning electron microscopy (SEM) micrographs for Br-2 and Cl-2, respectively, indicating that both Br-2 and Cl-2 samples have uniform particle size distributions and that the maximum dimension of particle size is about 1.0 μm. It should be mentioned that different batches can give similar size samples using this facile preparation approach (ESI,† Fig. S1).

The powder X-ray diffraction profiles over the 2θ range of 5–50° are shown in Fig. 2 and enlarged ones are displayed in Fig. 3. In comparison with the bulk crystals, broadening of the diffraction peaks is clearly seen in the diffraction profiles of the Br-2 and Cl-2 sub-micron crystals, owing to the reduction in crystal grain size. The diffraction pattern of the Br-2 sub-micron crystals is almost the same as that for the corresponding bulk crystals (Br-1); for instance, the diffraction peak positions, *e.g.* (110), (130), (200) and (220) and so on, are shifted only slightly to lower angle; however, these diffraction peaks are shifted obviously to lower angle in the powder X-ray diffraction profile of the Cl-2 sub-micron crystals, when compared with those in the corresponding bulk crystals (Cl-1). If the shift in the diffraction peaks to lower angle is the inherent nature of the Cl-2 sub-micron crystals, it means that lattice expansion occurs in the sub-micron crystals.

It is well-known that nanocrystals with free surfaces have considerable lattice contraction induced by the large surface/volume ratio,[9] and such a phenomenon is generally observed in metal nanocrystals.[10] In contrast with this common observation, lattice expansion as the particle size was reduced has also been found in some metal oxide nanocrystals.[11,12] Although the exact origin of the size-induced lattice expansion in metal oxide nanocrystals is still not clearly understood, the structural changes of the species on the nanocrystals surface are thought to play an important role in such a fairly surprising situation. For example, lattice expansion that has been observed in CeO_2 nanocrystals is thought to originate from the valence reduction of metal ions from Ce^{4+} to Ce^{3+} (which has a larger ionic radius) on the surface of the nanocrystals, with the increase in Ce–O bond lengths on the surface of the nanocrystals thought to result in the lattice expansion.[12] For Cl-1 and Cl-2, PXRD

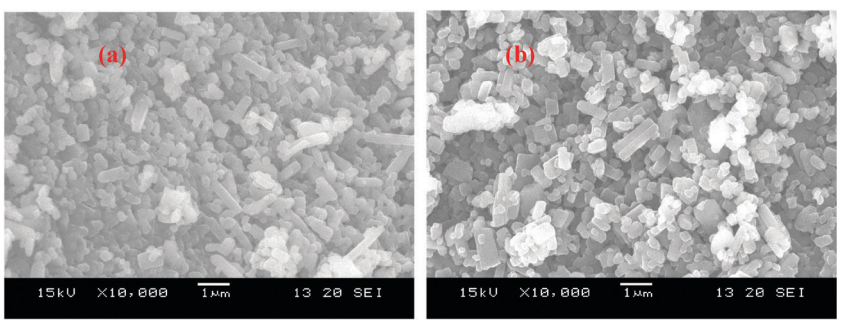

Fig. 1 SEM images of (a) Br-2 and (b) Cl-2.

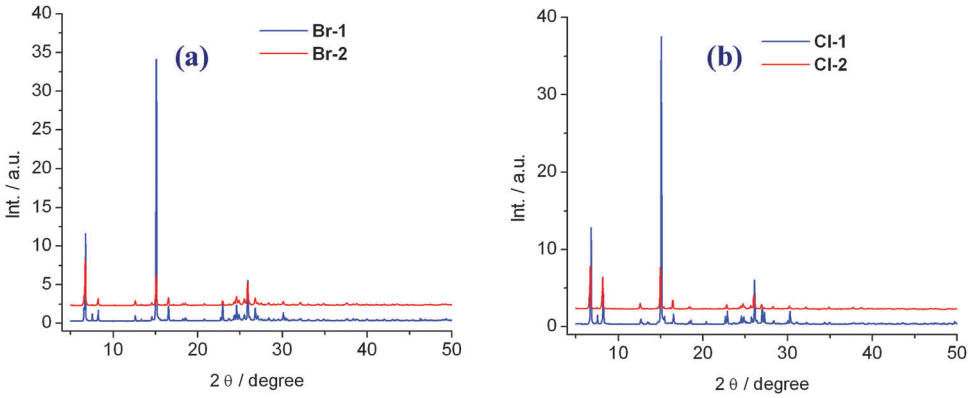

Fig. 2 Experimental powder X-ray diffraction profiles over the 2θ range of 5–50° for (a) Br-1 and Br-2, and (b) Cl-1 and Cl-2.

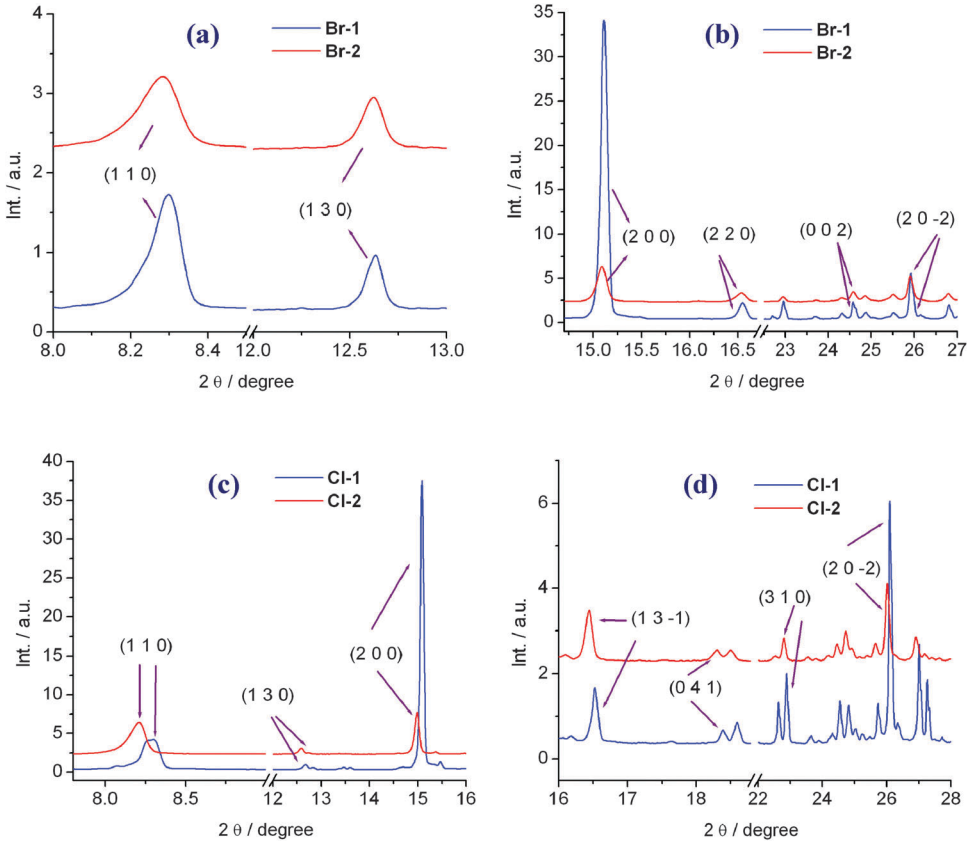

Fig. 3 Powder X-ray diffraction profiles at room temperature for (a, b) Br-1 and Br-2, and (c, d) Cl-1 and Cl-2.

measurements were performed using crystalline Si powder as an internal standard, shown in Fig. S2 in the ESI,† and the results disclosed that the small differences between the Cl-1 and Cl-2 PXRD patterns probably arise from the errors in the measurements.

Magnetic and spin-Peierls-type transition natures

The plots of χ_m–T are displayed in Fig. 4a and b for Br-1, Br-2, Cl-1 and Cl-2. Obvious distinctions are observed in the χ_m against T plots between those for the samples of sub-micron crystals and those for the corresponding bulk crystals, as follows: (1) the magnetic susceptibility changes sharply in the bulk crystals, whilst it is more rounded in the sub-micron crystal samples at the transition. An analogous phenomenon was reported in some spin-crossover (SCO) compounds, where downscaling the particles led to a more gradual magnetic susceptibility change in the thermal SCO process, owing to particle size-dependent cooperative interactions in the lattices of the SCO compounds.[13–18] (2) An onset of a strongly paramagnetic background appears in the sub-micron crystals, whereas diamagnetism (where negative magnetic susceptibility is clearly seen between 10 and 100 K for Br-1 and Cl-1) occurs in the corresponding bulk

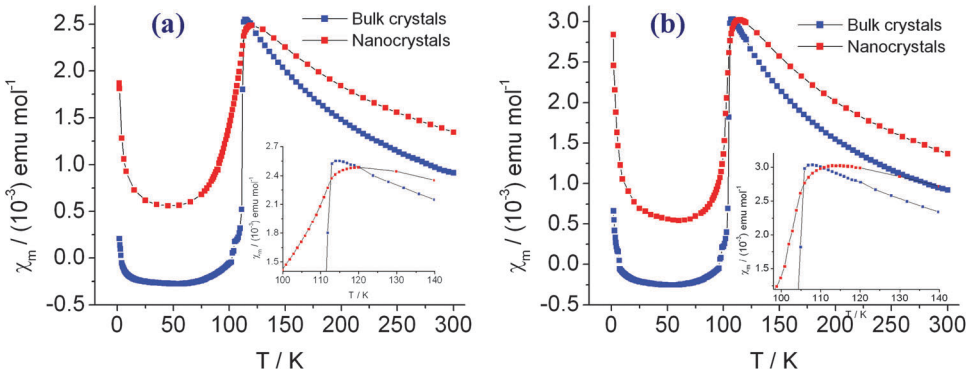

Fig. 4 Plots of χ_m–T of (a) Br-1 and Br-2, and (b) Cl-1 and Cl-2 (insets: enlarged plots).

crystals below the transition temperature. It is easily understandable that reducing the crystal size induces a strongly Curie–Weiss type paramagnetic background in such 1D magnetic systems, since an antiferromagnetic spin chain of $[Ni(mnt)_2]^-$ is decoupled at the position of the crystal surface. These decoupled $[Ni(mnt)_2]^-$ anions give a contribution to the Curie–Weiss type paramagnetic susceptibility, and a larger percentage of the decoupled $[Ni(mnt)_2]^-$ anions are at the surfaces of sub-micron crystals, owing to the larger surface/volume ratio in comparison with the bulk crystals.

Given that the spin gap opens below the magnetic transition in a 1D spin-Peierls system, the paramagnetic susceptibility contributed from the 1D magnetic chains is ignorable in the lower temperature region, owing to the existence of a big spin gap; as a result, the Curie–Weiss type paramagnetic background and the temperature-independent paramagnetism can be estimated from fits of the temperature-dependent magnetic susceptibilities in the lower temperature region using eqn (1):

$$\chi_m = \frac{C}{T-\theta} + \chi_0. \quad (1)$$

The first term in eqn (1) represents the Curie–Weiss type paramagnetic susceptibility; the parameters C and θ correspond to the Curie and Weiss constants, respectively. The parameter χ_0 is the summation of diamagnetism contributed from the cores of atoms in the molecules and the possible van Vleck-type temperature-independent paramagnetic susceptibility originating from the coupling of the ground and excited states through a magnetic field.[19] The fitted parameters of C, θ, χ_0 and the temperature range used for the fits are summarized in Table 1 for Br-1, Br-2, Cl-1 and Cl-2, indicating that only a 0.3% fraction of Curie–Weiss type paramagnetism for Br-1, *versus* ~0.7% for Cl-1, is estimated in the bulk crystals from the fitted Curie constants. However, pronounced Curie–Weiss type paramagnetism with a 1.1% fraction for Br-2, *versus* 2.1% for Cl-2, were observed in the sub-micron crystals (Table 1). Another striking feature which arose from the particle size reduction, when compared with the corresponding bulk crystal samples, is that temperature-independent paramagnetic susceptibilities appeared in the sub-micron crystal samples. For example, the fits to the magnetic susceptibility data gave negative χ_0 values for the bulk crystals Br-1 and Cl-1, moreover, the χ_0 values are close to the Pascal's constants of the corresponding 1D spin-Peierls-type compound; however, the positive χ_0 values for the sub-micron crystals Br-2 and Cl-2 demonstrate that van Vleck-type temperature-independent paramagnetic susceptibility exists in the sub-micron crystals.

Above the magnetic transition, from the structural viewpoint, the spin-Peierls-type compounds show the magnetic susceptibility character of a Heisenberg uniform antiferromagnetic chain. The corresponding magnetic susceptibility data were further analyzed using eqn (2) with eqn (3):

$$\chi_m = \chi_m(\text{chain}) + \frac{C}{T-\theta} + \chi_0 \quad (2)$$

$$\chi_m(\text{chain}) = \frac{Ng^2\mu_B{}^2}{k_B T} \cdot \frac{A + BX^{-1} + CX^{-2}}{1 + DX^{-1} + EX^{-2} + FX^{-3}}. \quad (3)$$

In eqn (2), the terms $C/(T-\theta)$ and χ_0 represent the Curie–Weiss type and temperature-independent magnetic susceptibilities,

Table 1 The fitted parameters and the temperature ranges used for both sub-micron crystals and bulk crystals

	Br-1	Br-2	Cl-1	Cl-2
In the low-temperature phase				
C/emu K mol^{-1}	1.07(3) × 10^{-3}	4.25(6) × 10^{-3}	2.61(13) × 10^{-3}	8.04(53) × 10^{-3}
θ/K	−0.06(6)	−1.16(4)	−0.61(14)	−1.61(22)
χ_0/emu mol^{-1}	−2.9(2) × 10^{-4}	4.6(4) × 10^{-4}	−3.1(7) × 10^{-4}	4.0(3) × 10^{-4}
Temp. range/K	2–50	2–45	2–50	2–55
In the high-temperature phase				
g	2.02(0)	2.0 (fixed)	2.0 (fixed)	1.9 (fixed)
$\lvert J\rvert/k_B$/K	13.4(4)	36(2)	2.3(1)	11(2)
Temp. range/K	128–300	140–300	124–300	140–300

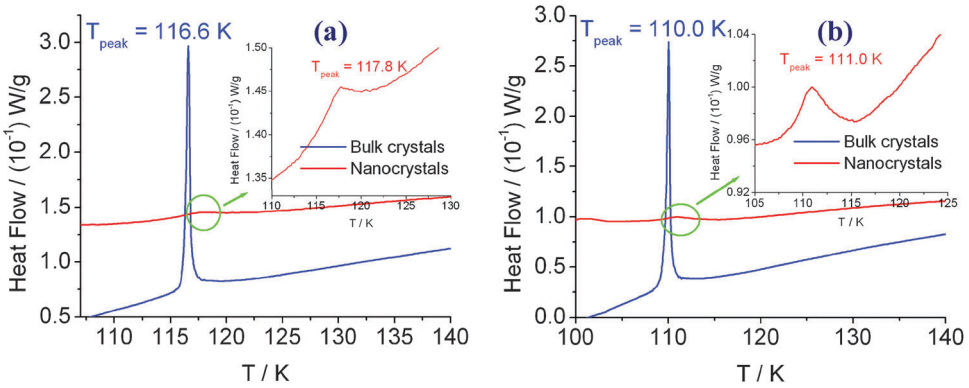

Fig. 5 DSC plots of (a) Br-1 and Br-2, and (b) Cl-1 and Cl-2.

respectively; the term χ_m(chain) corresponds to the magnetic susceptibility contributed from the magnetic chains, and eqn (3) is deduced from a $S = 1/2$ Heisenberg model of a uniform chain and is based on the spin Hamiltonian below:

$$\hat{H} = -2J\sum_{i=1}^{n}\hat{S}_{j-1}\hat{S}_j. \quad (4)$$

In eqn (3), $X = k_BT/|J|$, where J is the magnetic exchange constant of the neighboring spins in a uniform magnetic chain and the coefficients A–F are constants with the values $A = 0.25$, $B = 0.14995$, $C = 0.30094$, $D = 1.9862$, $E = 0.68854$ and $F = 6.0626$.[20]

In the fitting procedure, it was supposed that the Curie–Weiss type paramagnetic background and the temperature-independent paramagnetic term, χ_0, are the same in both the high- and low-temperature phases for each sample, and these terms were obtained from the fits to the magnetic susceptibility data in the low-temperature phase. The fitted magnetic exchange constant, J, and the temperature range used for the fits are listed in Table 1. It should be mentioned that the fit gave an unreasonable g-factor value for Br-1, so as a result, the g-factor value was fixed in the fitting process. The theoretically reproduced plots of χ_m–T match well with the experimental data for the bulk crystals (both Br-1 and Cl-1), whereas they do not match well for the sub-micron crystals (both Br-2 and Cl-2) in the high-temperature phase (ESI,† Fig. S3). The fits of the temperature-dependent magnetic susceptibility disclosed that the magnetic exchange constant (J) within a magnetic chain increases as the crystal particle size decreases in the high temperature phase.

The phenomenon that crystal grain size affects the phase transition or physical properties of a material has been observed in some ferroelectric or ferromagnetic systems. The well-known ferroelectric material $BaTiO_3$ experiences three-step structural phase transitions, namely, the cubic (C) → tetragonal (T) → orthorhombic (O) → rhombohedral (R) transition sequence. Arlt *et al.*[21] showed that in fine-grained (*ca.* 1 μm) polycrystalline samples, the O → T transition temperature shifts to higher temperatures with decreasing grain size. In $Sm_{0.5}Sr_{0.5}MnO_3$, Zhou *et al.*[22] found that all the nanoparticles show a first-order ferromagnetic transition under low magnetic fields, but a second-order one above a critical field, HCR. As the particle size decreases, the ferromagnetic transition temperature, the thermal hysteresis width in the magnetizations and HCR, as well as the Weiss constant θ_{PM} in the high-temperature paramagnetic phase exhibit a significant decrease, indicating that the ferromagnetism is weakened and the first-order transition is softened; such a phenomenon is due to the weakened double-exchange interactions and the strongly suppressed charge-ordered antiferromagnetic state by the reduction in size, respectively. In our 1D spin systems, the exact mechanism is not clear for the phenomenon of the crystal grain-dependent J at the present stage.

Differential scanning calorimetry (DSC) measurements were additionally performed to precisely determine the change of T_C for these 1D spin-Peierls-type systems, and the corresponding curves are shown in Fig. 5. The critical temperature of the transition, T_C, is upshifted with $\Delta T_C \approx 1.2$ K for Br-2 *versus ca.* 1.0 K for Cl-2, with respect to the bulk crystal samples.

Theoretically, the expression for the spin-Peierls transition temperature, T_C, is of the BCS form:

$$k_BT_C = 1.14(pJ)\exp(1/\lambda) \quad (5)$$

$$\lambda = 4g^2p^2N_0/{\omega_0}^2 \quad (6)$$

$$g = g(\lambda q,\ q = 2k_f), \quad (7)$$

where $N_0 = 1/pJ\pi$ is the density of states at k_f for the fermion band, J is the static exchange constant, and the only weakly temperature-dependent constant $p = 1.64$; ω_0 and g represent the phonon frequency in the absence of spin interaction and the spin–phonon coupling constant, respectively.[23,24] As a result, the spin-Peierls-type critical temperature, T_C, increases with the magnetic coupling interactions (J) within a magnetic chain. In our previous study, such a phenomenon of magnetic exchange constant (J)-dependent T_C was really observed. The T_C in a series of [1-(4′-R-benzyl)pyridinium][Pt(mnt)$_2$] salts was found to be much higher than those in the isostructural [1-(4′-R-benzyl)pyridinium][Ni(mnt)$_2$] salts with the same substituent R (R = Cl, Br, NO_2, CH_3, CH═CH_2), owing to the bigger J value in the $[Pt(mnt)_2]^-$ salt with respect to the corresponding $[Ni(mnt)_2]^-$ salt.[6a,b,25] Therefore, the fact that the sub-micron crystal samples show higher T_C values than the corresponding bulk crystal samples is probably related to their increased J values.

The enthalpies and entropies of the spin-Peierls-type transition, including the contribution of both structure and spin, are estimated as $\Delta H \approx 0.472$ kJ mol^{-1} and $\Delta S \approx 4.06$ J K^{-1} mol^{-1} for Br-1, *versus* $\Delta H \approx 0.537$ kJ mol^{-1} and $\Delta S \approx 4.88$ J K^{-1} mol^{-1} for Cl-1. The transition entropy contributed from the structure is almost equal to zero because the crystal structures are ordered in both the high- and the low-temperature phases. The estimated entropies of phase transition are lower than the theoretical maximum spin entropies from a mole of $S = 1/2$ anions in the HT phase to $S = 0$ anions in the LT phase ($R \ln 2 \approx 5.76$ J K^{-1} mol^{-1});[26] this suggests that a substantial short-range order persists above the magnetic transition temperature of Br-1 and Cl-1. The short-range order is an indication of a lowered dimensionality of the spin system,[27] and is consistent with the uniform chain structure of the $[Ni(mnt)_2]^-$ anions in the bulk crystals (Br-1 and Cl-1).[8] The enthalpies and entropies of the spin-Peierls-type transition are estimated as $\Delta H \approx 0.073$ kJ mol^{-1} and $\Delta S \approx 0.62$ J K^{-1} mol^{-1} for Br-2, *versus* $\Delta H \approx 0.031$ kJ mol^{-1} and $\Delta S \approx 0.27$ J K^{-1} mol^{-1} for Cl-2. Obviously, reducing the crystal grain size gives rise to the enthalpies and entropies of the spin-Peierls-type transition significantly decreasing. The phenomenon that the enthalpy and entropy of transition reduce with decreasing particle size was also reported in another phase transition material,[28] and the particle size-dependent enthalpy and entropy of transition is probably related to the lattice defects; in general, the lattice defects increase with decreasing particle size.

Conclusion and remarks

In summary, sub-micron crystals were prepared for two 1D $[Ni(mnt)_2]^-$-based spin-Peierls-type compounds. An up-shift in the magnetic transition temperature, the onset of a strongly Curie–Weiss type paramagnetic background and significant temperature-independent paramagnetism appear in the sub-micron crystals with respect to the bulk crystals. The strongly Curie–Weiss type paramagnetic background in the sub-micron crystals of the two 1D compounds is due to antiferromagnetic spin chains of $[Ni(mnt)_2]^-$ being decoupled at the position of the crystal surface. These decoupled $[Ni(mnt)_2]^-$ anions contribute to the Curie–Weiss type paramagnetic susceptibility, and a larger percentage of the $[Ni(mnt)_2]^-$ anions are on the surfaces of sub-micron crystals than for the bulk crystals. In addition, the size-dependent magnetic and phase transition behaviors further support the existence of a phonon confinement effect in 1D $[Ni(mnt)_2]^-$-based spin-Peierls-type compounds.

Acknowledgements

The authors thank the Priority Academic Program Development of Jiangsu Higher Education Institutions, Special Research Fund for the Doctoral Program of Higher Education and National Nature Science Foundation of China for financial support (grant no. 20123221110013 and 21271103).

References

1 (*a*) J. S. Biteen, N. S. Lewis, H. A. Atwater and A. Polman, *Appl. Phys. Lett.*, 2004, **84**, 5389; (*b*) Y. F. Li, A. J. Mao, Y. Li and X. Y. Kuang, *J. Mol. Model.*, 2012, **18**, 3061.
2 (*a*) V. Luca, *J. Phys. Chem. C*, 2009, **113**, 6367; (*b*) S. K. Sahoo, S. Pal, P. Sarkar and C. Majumder, *Chem. Phys. Lett.*, 2011, **516**, 68; (*c*) A. B. Moshe, D. Szwarcman and G. Markovich, *ACS Nano*, 2011, **5**, 9034; (*d*) B. Wei, K. Zheng, Y. Ji, Y. F. Zhang, Z. Zhang and X. D. Han, *Nano Lett.*, 2012, **12**, 4595.
3 (*a*) C. B. Murray, D. J. Norris and M. G. Bawendi, *J. Am. Chem. Soc.*, 1993, **115**, 8706; (*b*) A. P. Alivisatos, *Science*, 1996, **271**, 933; (*c*) H. Zeng, J. Li, J. P. Liu, Z. L. Wang and S. Sun, *Nature*, 2002, **420**, 395.
4 G. S. Li, J. Boerio-Goates, B. F. Woodfield and L. P. Li, *Appl. Phys. Lett.*, 2004, **85**, 2059.
5 Y. Wang and N. Herron, *J. Phys. Chem.*, 1991, **95**, 525.
6 (*a*) X. M. Ren, Q. J. Meng, Y. Song, C. S. Lu, C. J. Hu and X. Y. Chen, *Inorg. Chem.*, 2002, **41**, 5686; (*b*) Z. F. Tian, H. B. Duan, X. M. Ren, C. S. Lu, Y. Z. Li, Y. Song, H. Z. Zhu and Q. J. Meng, *J. Phys. Chem. B*, 2009, **113**, 8278; (*c*) H. B. Duan, X. M. Ren and Q. J. Meng, *Coord. Chem. Rev.*, 2010, **254**, 1509.
7 (*a*) X. M. Ren, T. Akutagawa, S. Noro, S. Nishihara, T. Nakamura, Y. Yoshida and K. Inoue, *J. Phys. Chem. B*, 2006, **110**, 7671; (*b*) X. M. Ren, S. Nishihara, T. Akutagawa, S. Noro, T. Nakamura, W. Fujita, K. Awaga, Z. P. Ni, J. L. Xie, Q. J. Meng and R. K. Kremer, *Dalton Trans.*, 2006, 1988.
8 G. J. Yuan, S. P. Zhao, C. Wang, X. M. Ren and J. L. Liu, *Chem. Commun.*, 2011, **47**, 9489.
9 (*a*) C. W. Mays, J. S. Vermaak and D. Kuhlmann-Wilsdorf, *Surf. Sci.*, 1968, **12**, 134; (*b*) H. J. Wasserman and J. S. Vermaak, *Surf. Sci.*, 1972, **32**, 168; (*c*) G. Apai and J. F. Hamilton, *Phys. Rev. Lett.*, 1979, **43**, 165; (*d*) Q. Jiang, L. H. Liang and D. S. Zhao, *J. Phys. Chem. B*, 2001, **105**, 6275.
10 A. Taneda and Y. Kawazoe, *J. Magn. Soc. Jpn.*, 1999, **23**, 679.
11 V. R. Palkar, P. Ayyub, S. Chattopadhyay and M. Multani, *Phys. Rev. B: Condens. Matter Mater. Phys.*, 1996, **53**, 2167.
12 S. Tsunekawa, K. Ishikawa, Z. Q. Li, Y. Kawazoe and A. Kasuya, *Phys. Rev. Lett.*, 2000, **85**, 3440.
13 I. Y. Barskaya, E. V. Tretyakov, R. Z. Sagdeev, V. I. Ovcharenko, E. G. Bagryanskaya, K. Yu. Maryunina, T. Takui, K. Sato and M. V. Fedin, *J. Am. Chem. Soc.*, 2014, **136**, 10132.
14 P. Durand, S. Pillet, E.-E. Bendeif, C. Carteret, M. Bouazaoui, H. E. Hamzaoui, B. Capoen, L. Salmon, S. Hebert, J. Ghanbaja, L. Arandah and D. Schaniel, *J. Mater. Chem. C*, 2013, **1**, 1933.
15 *Spin-Crossover Materials: Properties and Applications*, ed. M. A. Halcrow, John Wiley & Sons, Chichester, UK, 2013.
16 P. Gütlich and H. A. Goodwin, *Top. Curr. Chem.*, 2004, 233.
17 A. Bousseksou, G. Molnar, L. Salmon and W. Nicolazzi, *Chem. Soc. Rev.*, 2011, **40**, 3313.
18 J. Larionova, L. Salmon, Y. Guari, A. Tokarev, K. Molvinger, G. Molnar and A. Bousseksou, *Angew. Chem., Int. Ed.*, 2008, **47**, 8236.
19 J. H. van Vleck, *The Theory of Electric and Magnetic Susceptibilities*, Oxford, London, 1932.

20 (*a*) J. C. Bonner and M. E. Fisher, *Phys. Rev. A: At., Mol., Opt. Phys.*, 1964, **135**(3A), A640; (*b*) W. E. Hatfild, *J. Appl. Phys.*, 1981, **52**, 1985.
21 G. Arlt, D. Hennings and G. de With, *J. Appl. Phys.*, 1985, **58**, 1619.
22 S. M. Zhou, Y. Q. Guo, J. Y. Zhao, C. L. Wang, L. F. He and L. Shi, *J. Appl. Phys.*, 2012, **111**, 056104.
23 R. K. Kremer, R. W. Henn, A. Faißt, J. Wosnitza and H. V. Löhneysen, *Czech. J. Phys.*, 1996, **46**, 1977.
24 E. Pytte, *Phys. Rev. B: Solid State*, 1974, **10**, 4637.
25 (*a*) X. M. Ren, H. Okudera, R. K. Kremer, Y. Song, C. He, Q. J. Meng and P. H. Wu, *Inorg. Chem.*, 2004, **43**, 2569; (*b*) D. B. Dang, C. L. Ni, Y. Bai, Z. F. Tian, Z. P. Ni, L. L. Wen, Q. J. Meng and S. Gao, *Chem. Lett.*, 2005, **34**, 680; (*c*) W. H. Ning, X. R. Chen, J. L. Liu, H. Yang and X. M. Ren, *Dalton Trans.*, 2014, **43**, 2997; (*d*) W. H. Ning, L. Zhai and X. M. Ren, *Synth. Met.*, 2015, **199**, 255.
26 X. M. Ren, T. Akutagawa, S. Nishihara, T. Nakamura, W. Fujita and K. Awaga, *J. Phys. Chem. B*, 2005, **109**, 16610.
27 S. N. Bhatia, C. J. O'Connor, R. L. Carlin, H. A. Algra and L. J. DeJongh, *Chem. Phys. Lett.*, 1977, **50**, 353.
28 M. J. M. Van Oort and M. L. Cotton, *Thermochim. Acta*, 1993, **219**, 245.